ACS Catalysis
Research Article
pubs.acs.org/acscatalysis

Highly Efficient Activation, Regeneration, and Active Site Identification of Oxide-Based Olefin Metathesis Catalysts

Kunlun Ding,[†] Ahmet Gulec,[‡] Alexis M. Johnson,[†] Tasha L. Drake,[†] Weiqiang Wu,[§] Yuyuan Lin,[‡] Eric Weitz,[†] Laurence D. Marks,[‡] and Peter C. Stair[*,†,∥]

[†]Department of Chemistry, Northwestern University, Evanston, Illinois 60208, United States
[‡]Department of Materials Science and Engineering, Northwestern University, Evanston, Illinois 60208, United States
[§]Center for Catalysis and Surface Science, Northwestern University, Evanston, Illinois 60208, United States
[∥]Chemical Sciences & Engineering Division, Argonne National Laboratory, Argonne, Illinois, 60439 United States

Supporting Information

ABSTRACT: Supported metal oxide based olefin metathesis catalysts are widely used in the chemical industry. In comparison to their organometallic catalyst cousins, the oxide catalysts have much lower activity due to the very small fraction of active sites. We report that a simple pretreatment of MoO_3/SiO_2 and WO_3/SiO_2 under an olefin-containing atmosphere at elevated temperatures leads to a 100−1000-fold increase in the low-temperature propylene metathesis activity. The performance of these catalysts is comparable with those of the well-defined organometallic catalysts. Unprecedentedly, the catalyst can be easily regenerated by inert gas purging at elevated temperatures. Furthermore, using UV resonance Raman spectroscopy and electron microscopy, we provide strong evidence that the active sites for MoO_3/SiO_2 are derived from monomeric $Mo(=O)_2$ dioxo species.

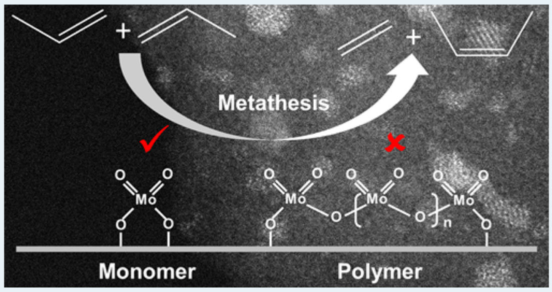

KEYWORDS: *olefin metathesis, metal oxides, active site, activation, regeneration*

■ INTRODUCTION

Supported metal oxide based olefin metathesis catalysts (MoO_x, WO_x, and ReO_x) have been widely used in megaton-scale industrial processes, including the Olefins Conversion Technology, the Shell Higher Olefin Process, etc.[1−3] Unfortunately, the activity of supported metal oxide catalysts is usually lower than that of organometallic catalysts by several orders of magnitude.[2,4] Extensive efforts have been devoted to integrating the merits of homogeneous organometallic catalysts' high activity and selectivity with that of supported metal oxide catalysts' ease of separation and regeneration. One approach is heterogenizing homogeneous olefin metathesis catalysts by grafting them on various supports. This technique improves the recyclability of these expensive organometallic compounds at the expense of catalytic activity.[4−7] Another approach is to enhance the activity of supported metal oxides either with promoters such as organotin compounds or with unusual and complicated pretreatments.[2,3,8−10] Supported organometallic catalysts and organotin-promoted supported metal oxides require complex syntheses and are not easily regenerated. Practically speaking, the development of highly effective pretreatment methods to improve the performance of supported metal oxide catalysts would be desirable. Conventional pretreatment in most metathesis studies includes high-temperature calcination and inert gas purging.[2,3] It has been shown that an olefin pretreatment at elevated temperature can improve the initial activity by shortening the induction period;[2,3,11−13] however, the overall increase in activity is rather modest. More effective pretreatment protocols that have also been reported include photoreduction by carbon monoxide[8,9] and reduction by atomic hydrogen at liquid nitrogen temperature,[10] but these procedures are not suitable for large-scale industrial applications. To the best of our knowledge, no Mo- or W-based heterogeneous olefin metathesis catalyst has been reported which simultaneously possesses high activity, selectivity, stability, and ease of regeneration.

The failure to develop such an ideal oxide-based olefin metathesis catalyst is largely due to an incomplete knowledge of the active site structures and how to generate them. Unlike the family of organometallic olefin metathesis catalysts that have well-defined structures, supported metal oxides always contain a mixture of surface species, where often less than 1−2% of the total metal atoms contribute to the reaction.[2,13−15] As a result, identifying and elucidating the structure of the active sites is an extremely challenging task.

Here we demonstrate that a very simple pretreatment of wet impregnated MoO_3/SiO_2 and WO_3/SiO_2 catalysts under an

Received: January 11, 2016
Revised: June 18, 2016

DOI: 10.1021/acscatal.6b00098
ACS Catal. 2016, 6, 5740−5746

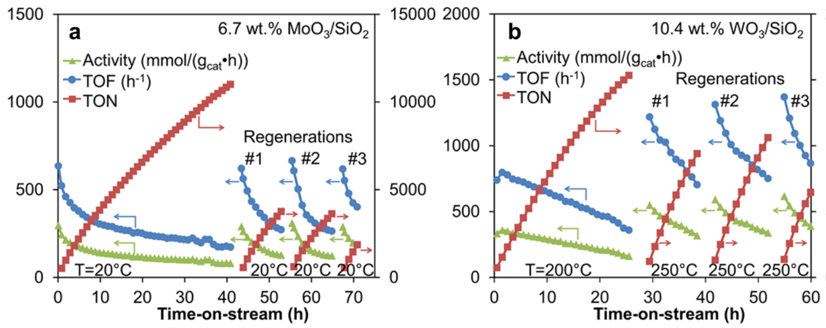

Figure 1. Time-on-stream propylene metathesis performance of MoO_3/SiO_2 (a) and WO_3/SiO_2 (b) after high-temperature activation procedures. A 100 mg portion of MoO_3/SiO_2 was activated in C_3H_6/N_2 = 4 sccm/96 sccm at 550 °C for 30 min and then purged with N_2 at 550 °C for 10 min; 100 mg of WO_3/SiO_2 was activated in C_3H_6/N_2 = 4 sccm/96 sccm, the temperature was increased from 550 to 700 °C with a ramp rate of 10 °C/min and kept at 700 °C for 30 min, and then the system was purged with N_2 at 700 °C for 10 min. The first regeneration was conducted via calcination in air up to 550 °C followed by reactivation in propylene as described above. The second and third regenerations were conducted via N_2 purging at 550 °C (Mo) or 700 °C (W) for 10 min. The reaction was conducted at 250 °C after the first regeneration of WO_3/SiO_2 to study the time-on-stream behavior of WO_3/SiO_2 at 250 °C, where the activity is higher than that at 200 °C.

olefin-containing atmosphere at elevated temperatures results in a 100−1000-fold increase in the low-temperature propylene metathesis activity. The observed activity, selectivity, and stability of our catalysts are comparable with those of high-performance supported organometallic catalysts. Unexpectedly, our catalysts can be regenerated simply by inert gas purging at elevated temperatures. Furthermore, the concentration of active sites correlates with both electron microscopy images and Raman spectroscopy bands of isolated $Mo(=O)_2$ species, suggesting that these species are the active site precursors on MoO_3/SiO_2 catalysts. This provides valuable guidance for the rational design of low-cost and high-performance oxide-based olefin metathesis catalysts relevant for many applications.[4,6,16]

RESULTS AND DISCUSSION

MoO_3/SiO_2 and WO_3/SiO_2 with different loadings were prepared via wet impregnation followed by drying and calcination (experimental details in the Supporting Information). Propylene metathesis was examined over these catalysts (reactor schematic shown in Figure S1 in the Supporting Information). Figures S2 and S3 in the Supporting Information show the temperature-programmed reaction spectra (TPRx) of MoO_3/SiO_2 and WO_3/SiO_2 after a conventional activation process which includes high-temperature calcination and inert gas purging.[2,3] Propylene conversion is negligible at low temperatures, but with increasing reaction temperature the conversion increases, reaches a plateau, then increases again, and finally reaches a maximum. In comparison to MoO_3/SiO_2, WO_3/SiO_2 requires higher activation temperatures to give an appreciable olefin metathesis activity because of its comparatively poor reducibility.[2,4] The TPRx showed progressive activation during the temperature-programmed reaction, which encouraged us to study the activation of MoO_3/SiO_2 and WO_3/SiO_2 by high-temperature propylene pretreatments.

The activation procedure was explored within the bounds of varying the propylene concentration and activation temperature (discussed later). The best result for MoO_3/SiO_2 was obtained via 4/96 (v/v) propylene/N_2 pretreatment at 550 °C for 30 min with an additional inert gas purge for 10 min at the same temperature. An activation temperature of 700 °C was used for WO_3/SiO_2. Figure 1 and Figures S4−S6 in the Supporting Information show the low-temperature propylene metathesis performance of MoO_3/SiO_2 and WO_3/SiO_2 after the optimized activation procedure. Propylene metathesis to produce ethylene and 2-butenes is a reversible reaction, with an equilibrium propylene conversion of 42% at 20 °C (calculated from HSC 5.1), which we approach but do not achieve. The products observed over the pretreated MoO_3/SiO_2 and WO_3/SiO_2 catalysts are exclusively ethylene and butenes, with a molar ratio close to 1. The selectivity toward 2-butenes out of the total butene products is greater than 99.5%, with isomerization products at less than 0.5%. The ratios of *cis*- to *trans*-2-butene are approximately 1/3 and 2/3 during the initial stage of reaction over MoO_3/SiO_2 (20 °C) and WO_3/SiO_2 (200 °C), respectively (Figures S5 and S6), which are very close to the equilibrium ratios at these reaction temperatures (calculated from HSC 5.1). We verified that the MoO_3/SiO_2 is also active for the reverse reaction, *cis*-2-butene + ethane to propylene (data not shown).

The initial turnover frequency (TOF calculation based on the total amount of metal) of MoO_3/SiO_2 at room temperature is approximately 640/h, equal to a weight-based activity of 300 mmol/(g_{cat} h). In the case of WO_3/SiO_2, the initial TOFs at 200 and 250 °C are 800/h and 1200/h, corresponding to 360 and 540 mmol/(g_{cat} h), respectively. The accumulated turnover number (TON) reaches 10000 within 40 and 10 h for MoO_3/SiO_2 and WO_3/SiO_2, respectively. These activities are 2−3 orders of magnitude higher than those when the catalysts are pretreated by calcination and inert gas purging alone. In comparison to the most active, reported MoO_3−Al_2O_3−SiO_2 catalysts made by flame synthesis (18 mmol/(g_{cat} h))[17] and aerosol synthesis (32 mmol/(g_{cat} h)),[18] our catalysts have 1 order of magnitude higher activity.

While the TOFs based on the total amount of Mo and W in the catalysts are comparable to those of high-performance supported organometallic catalysts (TOFs of 10^3−10^4/h),[4,5,19−23] when they are computed on an active site basis, evaluated below, the initial TOF of MoO_3/SiO_2 is 1.5×10^4/h. Previously, Blanc et al.[22] reported on a series of high-performance, organometallic-derived SiO_2-supported Mo-based olefin metathesis catalysts with propylene metathesis TOFs of 1.9×10^4/h to 4.8×10^4/h at 30 °C, values that are similar to ours.

The catalytic activity of MoO_3/SiO_2 and WO_3/SiO_2 can be fully restored via calcination followed by reactivation in propylene, since this mimics the original activation procedure, but to our surprise, simple inert gas purging at elevated temperatures (550 °C for MoO_3/SiO_2 and 700 °C for $WO_3/$

DOI: 10.1021/acscatal.6b00098
ACS Catal. 2016, 6, 5740−5746

SiO_2) also fully restores the catalytic activity. Catalysts regenerated with either method behave in a manner that is analogous to the freshly activated catalyst. To the best of our knowledge, this is the first report that inert gas purging can completely regenerate an olefin metathesis catalyst. Taking into account that none of the organometallic olefin metathesis catalysts can be easily regenerated, our discovery of a regeneration pathway is highly significant.

We have studied the activation and regeneration processes in some detail. The widely accepted Hérisson−Chauvin olefin metathesis mechanism involves metallocarbene and metallacyclobutane intermediates,[24,25] implying that the successful activation of supported-oxide-based olefin metathesis catalysts requires the conversion of metal oxo (M═O) species into metallocarbene or metallacyclobutane. Temperature-programmed reaction experiments showed that during activation the formation of CH_4, CO, and H_2 started at around 500 °C on MoO_3/SiO_2 and at around 600 °C on WO_3/SiO_2 (Figure 2 and Figure S7 in the Supporting Information), while the bare SiO_2 support gave negligible propylene conversion up to 700 °C (Figure S8 in the Supporting Information). The observation of these products implies that the activation of MoO_3/SiO_2 and WO_3/SiO_2 is consistent with a so-called pseudo-Wittig reaction (Scheme 1),[26,27] which converts Mo═O and W═O into Mo═CHR and W═CHR (R = H, CH_3), releasing unstable aldehydes. These aldehydes quickly decompose into the observed CH_4, CO, and H_2. The formations of benzene and excess ethylene are likely from dehydroaromatization and hydrogenolysis of C_3H_6, respectively. A decrease in the quantity of Mo═O and W═O structures from the activation process is confirmed by UV resonance Raman spectroscopy (Figure S9 in the Supporting Information).

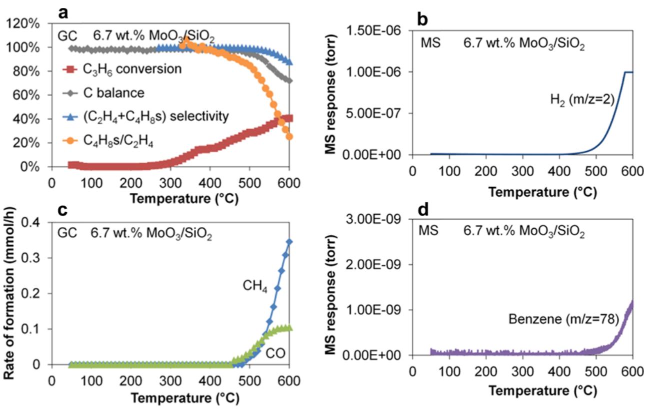

Figure 2. GC (a, c) and MS (b, d) analyses of the gaseous products generated during the temperature-programmed propylene metathesis over MoO_3/SiO_2. Reaction conditions: 200 mg of 6.7 wt % MoO_3/SiO_2; calcined in air (50 sccm) at 550 °C for 60 min; purged with N_2 (100 sccm) at 550 °C for 60 min; cooled to 50 °C under N_2 (100 sccm); switched to C_3H_6/N_2 = 4 sccm/96 sccm; temperature increased from 50 to 600 °C with a ramp rate of 1 °C/min.

Scheme 1. Possible Activation Mechanism and Side Reactions during the High-Temperature Olefin Pretreatment

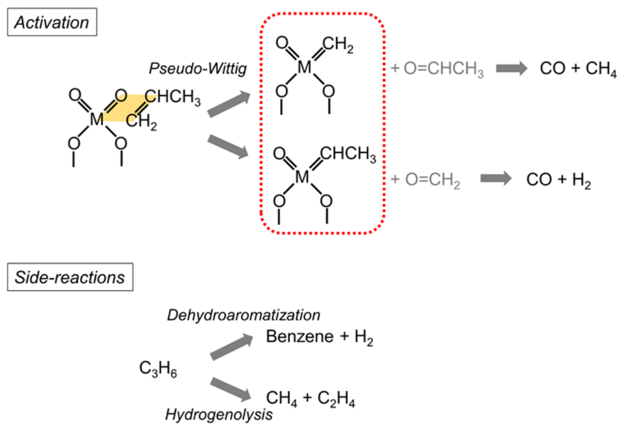

Although it has been known for some time that an olefin pretreatment would increase the initial activity of an oxide-based olefin metathesis catalyst by shortening its induction period,[2,13] a 2 orders of magnitude improvement in activity was not observed, because the pretreatment temperatures used were significantly lower than those in our work. Indeed, our measured activity was found to be sensitive to the pretreatment temperature, which needs to be close to 550 °C for MoO_x/SiO_2 and 700 °C for WO_x/SiO_2 in order to remove oxygen atoms and give rise to high activity (Figures 2 and 3 and Figure S7 in the Supporting Information). Increasing the propylene concentration from 4% to 50% for high-temperature activation of MoO_3/SiO_2 resulted in slightly lower activity at 20 °C (propylene conversion of 34.5% vs 28.2%). The generality of this approach was investigated by using ethylene instead of propylene for the activation, as well as different MoO_3 precursors and SiO_2 supports for the wet-impregnation synthesis of MoO_3/SiO_2. The high-temperature procedure led to similarly high catalytic performance. (Figure 3 and Figure S10 in the Supporting Information).

In order to gain a more in-depth understanding of the remarkable regeneration by inert gas purging, we used mass spectrometry (MS) to monitor the temperature-programmed desorption (TPD) process after deactivation of the MoO_3/SiO_2 catalyst at low reaction temperature. As shown in Figure 4a, ethylene, propylene, butene, and pentene signals were observed sequentially as the temperature increased. Desorption of these species was complete below 300 °C. They can be attributed to the decomposition of surface metallacyclobutanes with different branching structures. That desorption of these species coincides with the regeneration of active sites can be seen in the progressive regeneration at temperatures that correspond to their desorption temperatures (Figure 4b).

These results support the model that the low-temperature deactivation of MoO_3/SiO_2 in propylene metathesis follows an intrinsic mechanism. In addition to the Hérisson−Chauvin catalytic cycle, inactive states of the metallacyclobutanes have been implicated by both experimental and theoretical work.[20,28−30] With time-on-stream, most of the active structures gradually convert to energetically more stable but catalytically less active forms, resulting in catalyst deactivation. Upon inert gas purging at elevated temperatures, all types of structures in both active and inactive states decompose and restore the original active surface structures, and the catalyst is regenerated. Both cycloreversion and reductive elimination are involved in the decomposition process. The presence of reductive elimination is suggested by the formation of pentene species during TPD (Figure 4a), as cycloreversion only gives ethylene, propylene, and butenes. Furthermore, when it is taken into account that butene isomerization activity is rather low at 200 °C (Figure S4 in the Supporting Information) and the concentration of the desorbed olefin species is also very low

DOI: 10.1021/acscatal.6b00098
ACS Catal. 2016, 6, 5740−5746

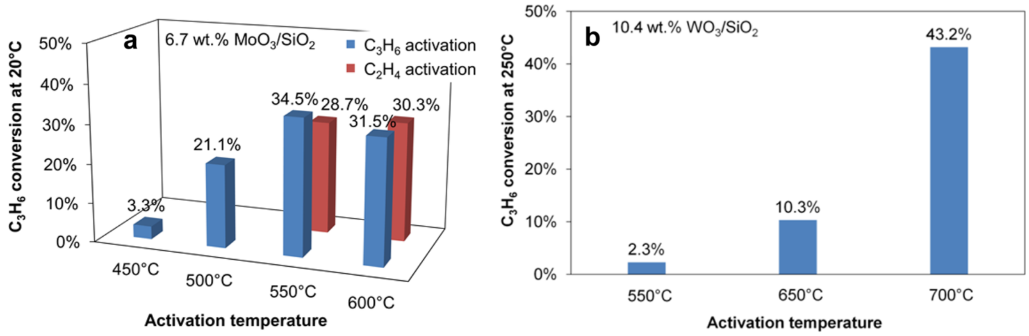

Figure 3. Propylene metathesis activity of MoO_3/SiO_2 (a) and WO_3/SiO_2 (b) activated in C_3H_6/N_2 or C_2H_4/N_2 at different temperatures. WO_3/SiO_2 was only activated in C_3H_6/N_2. Prior to activation, 200 mg of catalyst was calcined in air at 550 °C for 30 min and then purged with N_2 at 550 °C for 30 min. The catalyst was activated in C_3H_6/N_2 = 4 sccm/96 sccm at the target temperature for 30 min, purged with N_2 at the same temperature for 10 min, cooled to 20 °C (Mo) or 250 °C (W) in N_2, and switched to C_3H_6/N_2 = 40 sccm/5 sccm.

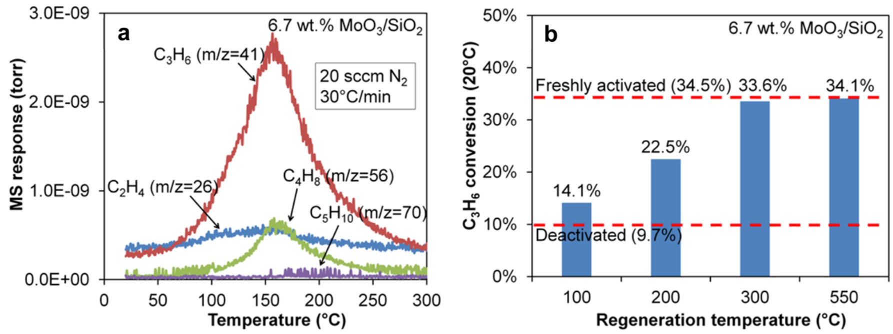

Figure 4. Regeneration of MoO_3/SiO_2 via inert gas purging: (a) TPD-MS of deactivated MoO_3/SiO_2; (b) propylene metathesis activity of MoO_3/SiO_2 recovered at different temperatures. The catalyst was deactivated in propylene metathesis at 100 °C for 1 h. Regeneration conditions: 20 sccm N_2; 30 °C/min from 20 °C to the target temperature and that temperature kept for 10 min.

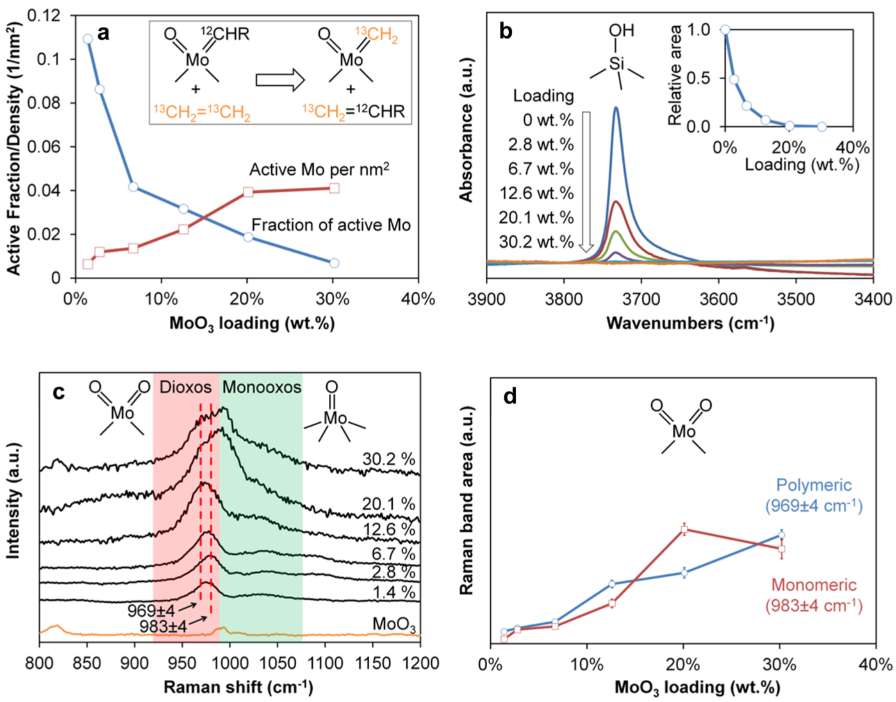

Figure 5. Olefin metathesis active site counting and structure identification in MoO_3/SiO_2: (a) MoO_3 loading dependent active site fraction and surface density from $^{13}CH_2{=}^{13}CH_2$ titration; (b) infrared and (c) UV resonance Raman spectra of MoO_3/SiO_2 with different loadings; (d) MoO_3 loading dependent Raman band areas of monomeric and polymeric molybdate dioxo species. The infrared spectra in (b) have been normalized to the amount of SiO_2. The Raman spectra in (c) have been normalized to the intensity of Si−O vibrations (400−700 cm^{-1}). The Raman band areas in (d) have been normalized to the surface areas of each MoO_3/SiO_2. The data in (d) represent the average values from multiple fittings by shifting the band positions ±1 cm^{-1} from the best-fitted positions; error bars represent standard deviations.

DOI: 10.1021/acscatal.6b00098
ACS Catal. 2016, 6, 5740−5746

Table 1. Results of Active Site Counting by $^{13}CH_2{=}^{13}CH_2$ Tracing

MoO_3 loading (wt %)	Mo coverage (per nm^2)	sample wt (mg)	$^{13}CH_2{=}^{12}CH_2$ (mmol)	$^{13}CH_2{=}^{12}CH^{12}CH_3$ (mmol)	fraction of active Mo	active Mo density (per nm^2)
1.4	0.059	300	0.00067	0.00256	10.9%	0.006
2.8	0.14	200	0.00108	0.00228	8.6%	0.012
6.7	0.35	200	0.00139	0.00250	4.2%	0.014
12.6	0.80	200	0.00172	0.00382	3.2%	0.022
20.1	2.6	200	0.00180	0.00344	1.9%	0.039
30.2	8.5	200	0.00112	0.00177	0.7%	0.041
6.7[a]	0.35	200	0	0	0	0
6.7[b]		200	0.00145	0.00378	5.6%	

[a]Pretreated by 550 °C calcination and nitrogen purge but without high-temperature propylene pretreatment. [b]MoO_3/SiO_2 catalyst prepared from $(NH_4)_2MoO_4$ precursor (surface area is not measured). Note that the amount of $^{13}CH_2{=}CHCH_3$ is always greater than that of $^{13}CH_2{=}CH_2$, indicating a higher activity of $Mo{=}CH_2$ in comparison to $Mo{=}CHCH_3$. This suggests that a great number of active site counting results reported in the literature were actually overestimated, as they only counted $Mo{=}CHCH_3$ and assumed that the amounts of $Mo{=}CH_2$ and $Mo{=}CHCH_3$ were equal.[13,15]

(butene concentration estimated less than 0.05% on the basis of our MS calibration), it is unlikely that the desorbed butenes can undergo secondary reactions such as isomerization and consecutive metathesis, which are needed for pentene formation by this route. Therefore, the most plausible route for pentene formation is reductive elimination of metallacyclobutanes. Empty sites generated from reductive elimination could combine with propylene to restore metallacyclobutane structures. Given the general nature of the deactivation mechanism, this type of regeneration should be universal for metal oxide based olefin metathesis catalysts.

Identification and characterization of catalytically active sites are prerequisites for an atomic-level understanding of the catalytic mechanism and rational design of high-performance heterogeneous catalysts. To this end, we counted the number of active sites of the pretreated MoO_3/SiO_2 by isotope tracing (detailed procedure described in the Supporting Information).[13,15] In brief, after the activated MoO_3/SiO_2 catalyst reached a steady state in propylene metathesis at room temperature, the system was thoroughly purged with nitrogen, followed by dosing with $^{13}CH_2{=}^{13}CH_2$. The formation of $^{13}CH_2{=}CH_2$ and $^{13}CH_2{=}CHCH_3$, originating from $Mo{=}CH_2$ and $Mo{=}CHCH_3$, respectively, was monitored by MS. A series of MoO_3/SiO_2 catalysts with different loadings were tested. The highest weight-base activity is 420 mmol/(g_{cat} h), which was obtained on the 12.6 wt % MoO_3/SiO_2 catalyst, as shown in Figure S11 in the Supporting Information. The active site counting results are given in Figure 5a and Table 1. The fraction of active Mo on the 6.7 wt % MoO_3/SiO_2 dramatically increases from close to 0 (negligible without a high-temperature propylene pretreatment) to 4.2% after a high-emperature propylene pretreatment. The fraction of Mo that is active increases as the loading of MoO_3 decreases and is maximized at 10.9% on the 1.4 wt % MoO_3/SiO_2 material. The fraction of active Mo obtained by this procedure is 10-fold higher than that of most supported MoO_3 catalysts.[15] This can explain, in part, the high activity of high-temperature, olefin-pretreated catalysts.

The surface density of active sites was calculated by normalizing the total number of active sites to the specific surface area of the catalyst, which was measured by N_2 sorption (Figures S12 and S13 in the Supporting Information). The specific surface area and pore volume (<150 nm) decrease with MoO_3 loading. Interestingly, the amount of larger-size mesopores (∼10 nm) increases with the expense of smaller-size mesopores (∼5 nm), which likely results from the restructuring of SiO_2 by MoO_3. As shown in Figure 5a, the surface density of active sites increases with MoO_3 loading and levels off beyond a loading of ca. 20 wt %. Infrared spectroscopy of MoO_3/SiO_2 shows that the silanols are almost completely consumed at 20 wt % (Figure 5b), implying that the molybdate species have saturated the SiO_2 surface at this loading. The formation of micron-sized MoO_3 crystals at 20 wt % is confirmed by X-ray diffraction and electron microscopy (Figures S14−S17 in the Supporting Information). UV−vis diffuse reflectance spectra show that the absorption band edge of the MoO_3/SiO_2 catalysts red-shifts with the MoO_3 loading (Figure S18 in the Supporting Information), indicating an increased average degree of polymerization of the molybdate species.[31] These measurements provide sample-averaged information. To identify the active site structure for olefin metathesis, techniques that can discriminate among different molybdate species are needed.

The distribution of molybdate species on the SiO_2 surface was studied by aberration-corrected high-angle annular dark-field (HAADF) imaging (Figure 6 and Figures S19−S21 in the Supporting Information). A mixture of monomeric, oligomeric, and clustered molybdates were observed over a broad range of loadings, and the population of all species increases with loading. Remarkably, clusters always appear to be the dominant surface species even at relatively low MoO_3 loadings, where silica-supported transition-metal oxides with low loadings are expected to be mostly monomeric species.[32,33] On the other hand, a significant quantity of monomeric molybdate species can be observed even at a loading as high as 20.1 wt %. These images are consistent with the hypothesis that the active sites

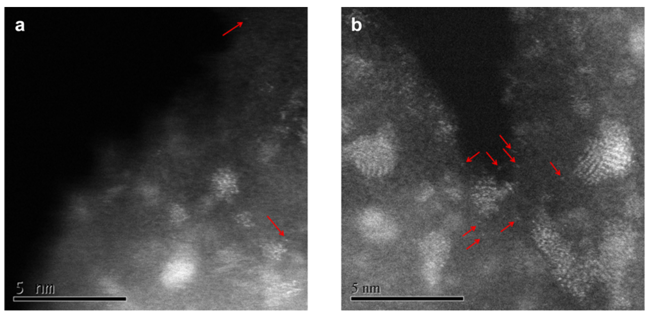

Figure 6. Aberration-corrected HAADF images of 2.8 wt % (a) and 20.1 wt % (b) of MoO_3/SiO_2 with arrows to mark the monomeric Mo. Scale bars are 5 nm.

DOI: 10.1021/acscatal.6b00098
ACS Catal. 2016, 6, 5740−5746

are derived from monomeric $Mo(=O)_2$ dioxo species that represent a small fraction of the surface Mo species.[5,17,18]

Raman spectroscopy is powerful for probing the molecular structure of supported metal oxides.[34] Great success has been achieved in identifying the catalytic site structures using this technique, including WO_x/ZrO_2 in alkane isomerization,[35,36] MoO_x/zeolite in methane dehydroaromatization,[37] etc. In comparison to normal Raman spectroscopy, resonance Raman spectroscopy can provide much higher sensitivity and selectivity in detecting surface metal oxide species even at low concentrations.[38,39] As shown in Figure 5c and Figure S22 in the Supporting Information, several bands appear in the region 950−1100 cm^{-1}, belonging to the Mo=O stretching vibration. According to the literature, bands above 990 cm^{-1} are assigned to Mo=O monooxo species.[28,31,33,40] On the basis of DFT calculations, the alkylidene derived from Mo=O monooxo sites is not expected to contribute to the metathesis activity because of high activation barriers for forming and decomposing the metallocyclobutane intermediate.[28] The bands below 990 cm^{-1} are assigned to a mixture of symmetric and asymmetric $Mo(=O)_2$ dioxo vibrations in monomeric and polymeric species.[28,31,33,40] The dramatic increase in the intensities of the bands below 990 cm^{-1} relative to the MoO_3 crystal band at 993 cm^{-1} in UV Raman (244 nm) vs visible Raman (488 nm) spectra of high-loading samples and the presence of Mo=O overtones under UV excitation indicate that the bands below 990 cm^{-1} are resonance-enhanced by more than 100-fold (Figures S22 and S23 in the Supporting Information). Since asymmetric vibrations do not belong to the totally symmetric point group, their resonance enhancement is weak or nonexistent[41] and they should not be visible in a UV resonance Raman spectrum. Therefore, the two bands at 983 ± 4 and 969 ± 4 cm^{-1} are assigned to the symmetric stretching modes of two distinct $Mo(=O)_2$ dioxo species, namely monomeric[28,31,33,40] and polymeric,[32,33] respectively (Figure 5c).

The peak areas of the Raman bands for monomeric and polymeric $Mo(=O)_2$ species shown in Figure 5c have been normalized to the specific surface area of each sample and plotted against the loading in Figure 5d and Figure S24 in the Supporting Information. As shown in Figure 5a,d, the area of the monomeric band correlates better with the changes in active site surface density than with the polymeric band, consistent with the conclusion that the active sites of MoO_3/SiO_2 in olefin metathesis are monomeric $Mo(=O)_2$ dioxo species. However, this conclusion cannot be said to be definitive. Both the electron microscopy and spectroscopy measurements were conducted on MoO_3/SiO_2 samples without high-temperature olefin pretreatment; at best these materials are precatalysts. Restructuring of surface molybdate species during the activation process, as shown in the MoO_x/zeolite system for methane dehydroaromatization,[37] cannot be excluded. In situ or operando studies of the catalyst speciation during the activation process would be highly desirable.

The monomeric nature of the metathesis active sites in supported MoO_x catalysts has been previously suggested on the basis of the relatively high activity of highly dispersed MoO_x synthesized through grafting, flame synthesis, and aerosol synthesis;[5,17,18] to the best of our knowledge, this is the first time the isolated $Mo(=O)_2$ species have been directly imaged and shown to have a positive, semiquantitative correlation with the surface density of active sites. On the basis of these results, the successful syntheses of predominantly monomeric $Mo(=O)_2$ dioxo species would be expected to greatly improve the olefin metathesis activity for supported MoO_x catalysts. Similar conclusions are expected for WO_x- and ReO_x-based olefin metathesis catalysts.

■ CONCLUSIONS

We have demonstrated that a simple pretreatment of MoO_3/SiO_2 and WO_3/SiO_2 under an olefin-containing atmosphere at elevated temperatures leads to a 100−1000-fold increase in the low-temperature propylene metathesis activity. The specific activity of these catalysts is comparable with those of the well-defined organometallic catalysts. Activation temperature thresholds were identified, which explains why previous studies using olefin pretreatment did not reach similarly high activity. We discovered that the deactivated catalysts can be easily regenerated by purging with inert gas at elevated temperatures. Examination of the desorbed species shows that the deactivation at low temperatures is likely due to the formation of stable, inactive metallacyclobutanes. Furthermore, we have shown a strong correlation between the population of active sites and monomeric $Mo(=O)_2$ dioxo species through a combination of isotope tracing, UV resonance Raman spectroscopy, and atomic-resolution electron microscopy.

■ ASSOCIATED CONTENT

Supporting Information

The Supporting Information is available free of charge on the ACS Publications website at DOI: 10.1021/acscatal.6b00098.

Materials and methods and Figures S1−S24 described in the text (PDF)

■ AUTHOR INFORMATION

Corresponding Author

*E-mail for P.C.S.: pstair@northwestern.edu.

Notes

The authors declare no competing financial interest.

■ ACKNOWLEDGMENTS

We acknowledge funding from the U.S. National Science Foundation CHE-1058835 (K.D., A.M.J., and P.C.S.), Northwestern University ISEN Booster Awards (K.D. and P.C.S.), Northwestern University Institute for Catalysis in Energy Processes (ICEP) on Grant DOE DE-FG02-03-ER15457 (K.D., A.G., W.W., Y.L., E.W., L.D.M., and P.C.S.). T.L.D. thanks the NSF for the award of a Graduate Research Fellowship. This work made use of the JEOL JEM-ARM200CF instrument in the Electron Microscopy Service (Research Resources Center, UIC). The acquisition of the UIC JEOL JEM-ARM200CF instrument was supported by an MRI-R2 grant from the National Science Foundation (DMR-0959470). This work also made use of the EPIC facility and Keck-II facility of the NUANCE Center and the J. B. Cohen X-ray Diffraction Facility at Northwestern University, which has received support from the MRSEC program (NSF DMR-1121262) at the Materials Research Center; the International Institute for Nanotechnology (IIN), the Keck Foundation, and the State of Illinois, through the IIN. We also acknowledge the Keck Biophysics Facility at Northwestern University.

■ REFERENCES

(1) Mol, J. C. *J. Mol. Catal. A: Chem.* **2004**, *213*, 39.
(2) Lwin, S.; Wachs, I. E. *ACS Catal.* **2014**, *4*, 2505.

(3) Mol, J. C.; van Leeuwen, P. W. N. M. *Handbook of Heterogeneous Catalysis* **2008**, *14*, 3240.
(4) Popoff, N.; Mazoyer, E.; Pelletier, J.; Gauvin, R. M.; Taoufik, M. *Chem. Soc. Rev.* **2013**, *42*, 9035.
(5) Iwasawa, Y.; Ichinose, H.; Ogasawara, S.; Soma, M. *J. Chem. Soc., Faraday Trans. 1* **1981**, *77*, 1763.
(6) Coperet, C.; Chabanas, M.; Saint-Arroman, R. P.; Basset, J. M. *Angew. Chem., Int. Ed.* **2003**, *42*, 156.
(7) Coperet, C. *Dalton Trans.* **2007**, 5498.
(8) Shelimov, B. N.; Elev, I. V.; Kazansky, V. B. *J. Catal.* **1986**, *98*, 70.
(9) Vikulov, K. A.; Shelimov, B. N.; Kazansky, V. B. *J. Mol. Catal.* **1991**, *65*, 393.
(10) Kazuta, M.; Tanaka, K. I. *J. Chem. Soc., Chem. Commun.* **1987**, 616.
(11) Yide, X.; Xinguang, W.; Yingzhen, S.; Yihua, Z.; Xiexian, G. *J. Mol. Catal.* **1986**, *36*, 79.
(12) Basrur, A. G.; Patwardhan, S. R.; Vyas, S. N. *J. Catal.* **1991**, *127*, 86.
(13) Amakawa, K.; Wrabetz, S.; Krohnert, J.; Tzolova-Muller, G.; Schlogl, R.; Trunschke, A. *J. Am. Chem. Soc.* **2012**, *134*, 11462.
(14) Chauvin, Y.; Commereuc, D. *J. Chem. Soc., Chem. Commun.* **1992**, 462.
(15) Handzlik, J.; Ogonowski, J. *Catal. Lett.* **2003**, *88*, 119.
(16) Hoveyda, A. H.; Zhugralin, A. R. *Nature* **2007**, *450*, 243.
(17) Debecker, D. P.; Schimmoeller, B.; Stoyanova, M.; Poleunis, C.; Bertrand, P.; Rodemerck, U.; Gaigneaux, E. M. *J. Catal.* **2011**, *277*, 154.
(18) Debecker, D. P.; Stoyanova, M.; Colbeau-Justin, F.; Rodemerck, U.; Boissiere, C.; Gaigneaux, E. M.; Sanchez, C. *Angew. Chem., Int. Ed.* **2012**, *51*, 2129.
(19) Chabanas, M.; Baudouin, A.; Coperet, C.; Basset, J. M. *J. Am. Chem. Soc.* **2001**, *123*, 2062.
(20) Salameh, A.; Baudouin, A.; Soulivong, D.; Boehm, V.; Roeper, M.; Basset, J. M.; Coperet, C. *J. Catal.* **2008**, *253*, 180.
(21) Mazoyer, E.; Szeto, K. C.; Merle, N.; Norsic, S.; Boyron, O.; Basset, J. M.; Taoufik, M.; Nicholas, C. P. *J. Catal.* **2013**, *301*, 1.
(22) Blanc, F.; Berthoud, R.; Salameh, A.; Basset, J. M.; Coperet, C.; Singh, R.; Schrock, R. R. *J. Am. Chem. Soc.* **2007**, *129*, 8434.
(23) Blanc, F.; Thivolle-Cazat, J.; Basset, J. M.; Coperet, C.; Hock, A. S.; Tonzetich, Z. J.; Schrock, R. R. *J. Am. Chem. Soc.* **2007**, *129*, 1044.
(24) Herisson, J. L.; Chauvin, Y. *Makromol. Chem.* **1971**, *141*, 161.
(25) Chauvin, Y. *Angew. Chem., Int. Ed.* **2006**, *45*, 3740.
(26) Rappe, A. K.; Goddard, W. A. *J. Am. Chem. Soc.* **1982**, *104*, 448.
(27) Grunert, W.; Stakheev, A. Y.; Feldhaus, R.; Anders, K.; Shpiro, E. S.; Minachev, K. M. *J. Catal.* **1992**, *135*, 287.
(28) Handzlik, J. *J. Phys. Chem. C* **2007**, *111*, 9337.
(29) Poater, A.; Solans-Monfort, X.; Clot, E.; Coperet, C.; Eisenstein, O. *J. Am. Chem. Soc.* **2007**, *129*, 8207.
(30) Handzlik, J.; Sautet, P. *J. Catal.* **2008**, *256*, 1.
(31) Lee, E. L.; Wachs, I. E. *J. Phys. Chem. C* **2007**, *111*, 14410.
(32) Banares, M. A.; Hu, H. C.; Wachs, I. E. *J. Catal.* **1994**, *150*, 407.
(33) Mestl, G.; Srinivasan, T. K. K. *Catal. Rev.: Sci. Eng.* **1998**, *40*, 451.
(34) Wachs, I. E.; Roberts, C. A. *Chem. Soc. Rev.* **2010**, *39*, 5002.
(35) Ross-Medgaarden, E. I.; Knowles, W. V.; Kim, T.; Wong, M. S.; Zhou, W.; Kiely, C. J.; Wachs, I. E. *J. Catal.* **2008**, *256*, 108.
(36) Zhou, W.; Ross-Medgaarden, E. I.; Knowles, W. V.; Wong, M. S.; Wachs, I. E.; Kiely, C. J. *Nat. Chem.* **2009**, *1*, 722.
(37) Gao, J.; Zheng, Y. T.; Jehng, J. M.; Tang, Y. D.; Wachs, I. E.; Podkolzin, S. G. *Science* **2015**, *348*, 686.
(38) Wu, Z. L.; Kim, H. S.; Stair, P. C.; Rugmini, S.; Jackson, S. D. *J. Phys. Chem. B* **2005**, *109*, 2793.
(39) Kim, H.; Kosuda, K. M.; Van Duyne, R. P.; Stair, P. C. *Chem. Soc. Rev.* **2010**, *39*, 4820.
(40) Tsilomelekis, G.; Boghosian, S. *Catal. Sci. Technol.* **2013**, *3*, 1869.
(41) Clark, R. J. H.; Stewart, B. *Struct. Bonding (Berlin, Ger.)* **1979**, *36*, 1.

DOI: 10.1021/acscatal.6b00098
ACS Catal. 2016, 6, 5740−5746